

The First Principle Study of the Structural, Electronic, Magnetic and Mechanical Properties of $\text{Fe}_{2-x}\text{Co}_x\text{TiSi}$ ($x=0, 0.5, 1, 1.5, 2$) Full Heusler Alloy

K. Rajesh Kanna¹, R. Rajeshwarapalanichamy²

¹Lecturer, Department of Physics, Lakshmi Ammal Polytechnic College, Kovilpatti

²Professor, Department of Physics, NMSSVN College, Madurai

Abstract: Investigation of the Structural, Electronic, Magnetic and Mechanical properties of the $\text{Fe}_{2-x}\text{Co}_x\text{TiSi}$ ($x = 0.0, 0.5, 1.0, 1.5, 2.0$) compounds in both the Hg_2CuTi and Cu_2MnAl -type structures using the first-principles density functional calculations, were studied by the augmented waves method. The exchange and correlation potential is treated by the generalized gradient approximation parameterized by Perdew-Burke-Erzerhof (GGA-PBE) and GGA-PBE+U scheme is used based on Dudarev's approach. The results show that the Cu_2MnAl -type structure is energetically more stable than the Hg_2CuTi -type structure for the Fe_2TiSi and Co_2TiSi compounds at the equilibrium volume. The substitution of Co atom in Fe_2TiSi for Fe, changes the semiconducting behavior to half metallic behavior in $\text{Fe}_{1.5}\text{Co}_{0.5}\text{TiSi}$, $\text{Fe}_{1.0}\text{Co}_{1.0}\text{TiSi}$, $\text{Fe}_{0.5}\text{Co}_{1.5}\text{TiSi}$ and Co_2TiSi . The magnetic properties for this full Heusler alloys upon substitution approach remains largely unexplored. It is worth noting that Fe_2TiSi alloy becomes magnetized after the introduction of Co atom. The mechanical properties of bulk modulus, shear modulus, Young's modulus E , anisotropic ratio, Poisson's ratio m and B/G ratio are also investigated to explore the ductile and brittle nature of these compounds.

1. Introduction

Experimentally, both Fe_2TiSi and Co_2TiSi based alloys were analysed [1-4] and it was found that Fe_2TiSi is non magnetic semiconductor and Co_2TiSi is half metallic ferromagnetic material. Voronin et al. [2] analyzed thermal properties of $\text{Fe}_2\text{TiSn}_{1-x}\text{Si}_x$.

The electronic properties of $\text{Fe}_2\text{TiSn}_{1-x}\text{Si}_x$ investigated. Bhat et al. [5] predicted the semiconducting behavior in Fe_2TiSi Heusler alloys with the band gap of 0.38 eV. Jong et al. [6] investigated the electronic properties of Fe_2TiSi and Fe_2TiSn alloys under pressure and they predicted that both the alloys are semiconductors.

The variation of band gap is analyzed by substituting Sn for Si in Fe_2TiSi ($\text{Fe}_2\text{TiSi}_{1-x}\text{Sn}_x$) using first principles calculations [7]. Yabuuchi et al. [8] have studied the electronic structure of full Heusler alloys with valence electron count of 24 (Fe_2TiSi and Fe_2TiSn) and these alloys were predicted as semiconductors. Sharma et al. [10] predicted that Co_2TiSi , Co_2TiGe and Co_2TiSn compounds are half metallic ferromagnetic materials with the magnetic moment $2 \mu_B$. The magnetic and electronic properties of Co_2TiSi and Co_2TiSn Heusler alloys were analysed using LSDA+U method by Zayed et al. [11]. From the above mentioned literature, it is seen that there is no substitution approach in the concerned Fe- based full Heusler alloys (i.e., Fe_2TiSi). Fe_2TiSi is found to be non- magnetic.

A solid body which is subject to external forces, or a body in which one part exerts a force on neighboring parts, is in a state of stress. If such forces are proportional to the area of the surface of the given part, the force per unit area is called the stress. The stress in a crystalline material is a direction dependent quantity and therefore, it is in general described by the stress tensor σ_{ij} . If all parts of the body

are in equilibrium and body forces are absent, the condition

$$\frac{\partial \sigma_{ij}}{\partial x_j} = 0 \text{ must be fulfilled. The symbols } x_j \text{ denote}$$

the cartesian axes. The deformations of the solid caused by the exerted stress are described by the strain tensor. If u_i is the displacement of a point x_j in a deformed solid, the strain tensor is then defined as

$$\epsilon_{ij} = \frac{1}{2} \left(\frac{\partial u_i}{\partial x_j} + \frac{\partial u_j}{\partial x_i} \right)$$

The diagonal components ϵ_{11} , ϵ_{22} and ϵ_{33} are called tensile strains, whereas the other components are usually denoted as shear strains. Both stress and strain tensors are symmetrical Hence I investigate the structural stability, electronic and magnetic properties of $\text{Fe}_{2-x}\text{Co}_x\text{TiSi}$ ($x = 0.0, 0.5, 1.0, 1.5, 2.0$) full Heusler alloys.

2. Computational Details

The ab initio calculations are performed using density functional theory within the generalized gradient approximation parameterized by Perdew-Burke-Erzerhof (GGA-PBE) [12-14] as implemented in the VASP code [15-17]. The interaction between the ion and electron is described by the projector augmented wave method [13]. Ground state geometries are determined by minimizing stresses and Hellmann-Feynman forces using conjugate-gradient algorithm with force convergence less than 10^{-3} eV \AA^{-1} and the Brillouin zone integration is performed with a Gaussian broadening of 0.1 eV. The Khon-Sham orbitals are expanded using the plane wave energy cutoff of 500 eV.

The Brillouin zone integrations are carried out using Monkhorst-Pack K-point mesh [18] with a grid size of $6 \times 6 \times 6$ for the total energy calculation. The valence electron

configurations are Fe 3d⁶ 4s², Co 3d⁷ 4s², 3d² 4s², Ti and 3s² 3p² of Si atoms. In order to correct the effect of strong correlation of 3d orbital of Fe, Co and Ti atoms, GGA-PBE+U scheme is used based on Dudarev's approach ($U_{\text{eff}} = U - J$) to address the onsite Coulomb interaction. The U-parameter value corresponding to minimum energy is found to be U= 1.8 eV for Fe, U= 2.0 eV for Co, U = 2.05 eV for Ti and exchange parameter J = 0.73 eV.

3. Result and Discussion

3.1 Structural Properties

The structural properties of the full Heusler alloys X₂YZ, with the combination of 3d elements of transition metals X= Fe, Co, Y= Ti and main group element Z= Si are analyzed. The total energies are computed for L₂₁ and XA phases of Fe₂TiSi and Co₂TiSi Heusler alloys. The structural stability between L₂₁ phase and XA phase is analyzed by plotting total energy (eV) values against cell volume (Å³) for (a) Fe₂TiSi and (b) Co₂TiSi, in Figure 3.1.1 and Figure 3.1.2. It is found that L₂₁ phase has the lower energy compared to XA phase. Thus, L₂₁ phase is predicted as the stable phase for both the alloys. Subsequently, all the total energy calculations are performed for Fe_{2-x}Co_xTiSi (x = 0.0, 0.5, 1.0, 1.5, 2.0) with L₂₁ phase. Table 3.1.3 shows the calculated ground state properties of Fe_{2-x}Co_xTiSi (x = 0.0, 0.5, 1.0, 1.5, 2.0) in L₂₁ structure with GGA- PBE and GGA- PBE+U calculations in addition to the available experimental and theoretical results [1,2, 4-6].

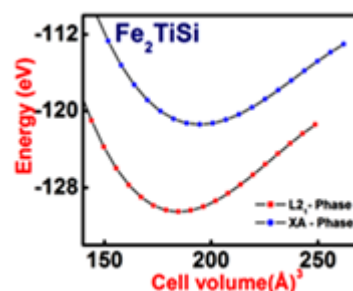


Figure 3.1.1: The structural stability between L₂₁ phase and XA phase is analyzed by plotting total energy (eV) values against cell volume (Å³) for Fe₂TiSi

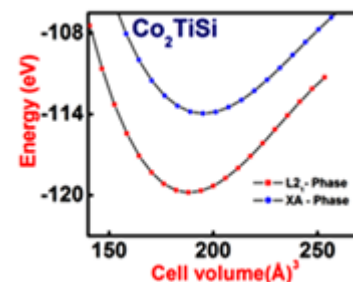


Figure 3.1.2: The structural stability between L₂₁ phase and XA phase is analyzed by plotting total energy (eV) values against cell volume (Å³) for Co₂TiSi

Table 3.1.3 calculated lattice parameters a (Å), equilibrium volume V₀ (Å³), formation enthalpy ΔH (eV), bulk modulus B (GPa) and its derivatives B₀' of Fe_{2-x}Co_xTiSi of considered L₂₁ structure using GGA- PBE and GGA PBE+U method.

	Method	A	V ₀	E	ΔH	B ₀	B ₀ '
Fe ₂ TiSi	GGA-PBE	5.6902	184.24	-130.426412	-9.824217	203.67	5.3786
	GGA-PBE+U	5.7209	187.24	-124.137768	-8.252056	197.99	5.3878
		5.658 ^a , 5.70 ^b , 5.658 ^{c,d} , 5.685 ^e				234.84 ^b , 232.098 ^c	4.51 ^b
Fe _{1.5} Co _{0.5} TiSi	GGA-PBE	5.6995	185.14	-127.546708	-10.458665	198.73	5.3808
	GGA-PBE+U	5.7376	188.88	-122.959203	-9.311789	190.64	5.3791
Fe _{1.0} Co _{1.0} TiSi	GGA-PBE	5.7022	185.41	-124.520830	-11.056570	199.02	5.3800
	GGA-PBE+U	5.7562	190.73	-119.922308	-9.906940	186.40	5.3792
Fe _{0.5} Co _{1.5} TiSi	GGA-PBE	5.7172	186.87	-122.168890	-11.962444	192.50	5.3811
	GGA-PBE+U	5.7575	190.85	-117.529125	-10.663018	179.46	5.3810
Co ₂ TiSi		5.7260					
	GGA-PBE	5.7803	187.74	-119.695878	-12.559081	194.60	5.3842
	GGA-PBE+U	5.743 ^f	193.13	-113.050861	-10.897827	186.52	5.3778
		5.760 ^g					
		5.6393 ^h					

^aRef [1] Expt, ^bRef [5] Theo, ^cRef [6] Theo, ^dRef [7] Theo, ^eRef [8] Theo, ^fRef [3] Expt, ^gRef [9] Theo, ^hRef [11] Theo

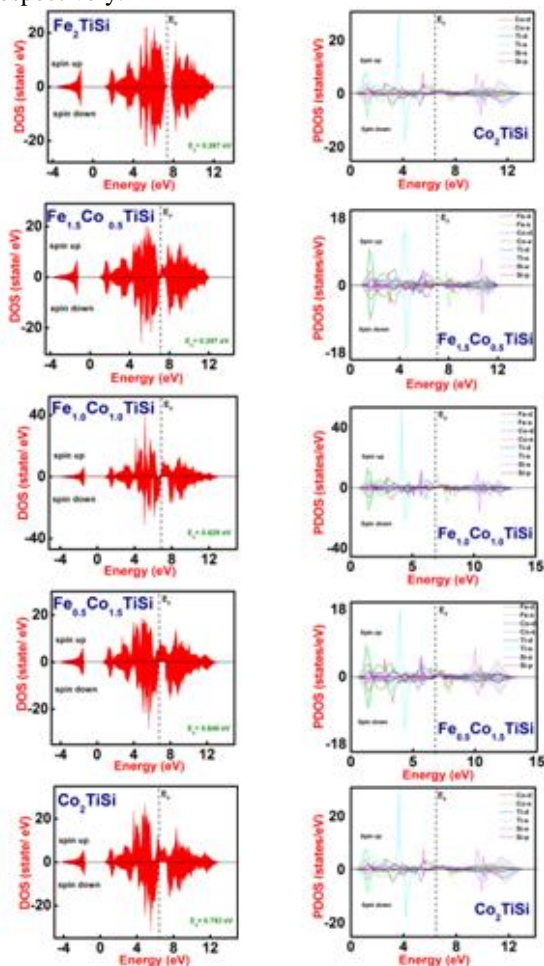
3.2 Electronic Properties

The electronic structure of full Heusler alloys Fe₂TiSi, Fe_{1.5}Co_{0.5}TiSi, Fe_{1.0}Co_{1.0}TiSi, Fe_{0.5}Co_{1.5}TiSi and Co₂TiSi is investigated by computing the spin polarized total and partial density of states (DOS) with GGA- PBE and GGA-PBE+U approach. The density of states computed with GGA- PBE scheme indicates semiconducting behavior for Fe₂TiSi [1,5-8] and half metallic nature for Fe_{1.5}Co_{0.5}TiSi, Fe_{1.0}Co_{1.0}TiSi, Fe_{0.5}Co_{1.5}TiSi and Co₂TiSi [9-11] full Heusler alloys. When, Co is substituted in Fe₂TiSi, the half metallicity is observed in

Fe_{1.5}Co_{0.5}TiSi, Fe_{1.0}Co_{1.0}TiSi, Fe_{0.5}Co_{1.5}TiSi and Co₂TiSi. The energy gap and spin flip gap values are enhanced while calculated using GGA- PBE+U scheme.

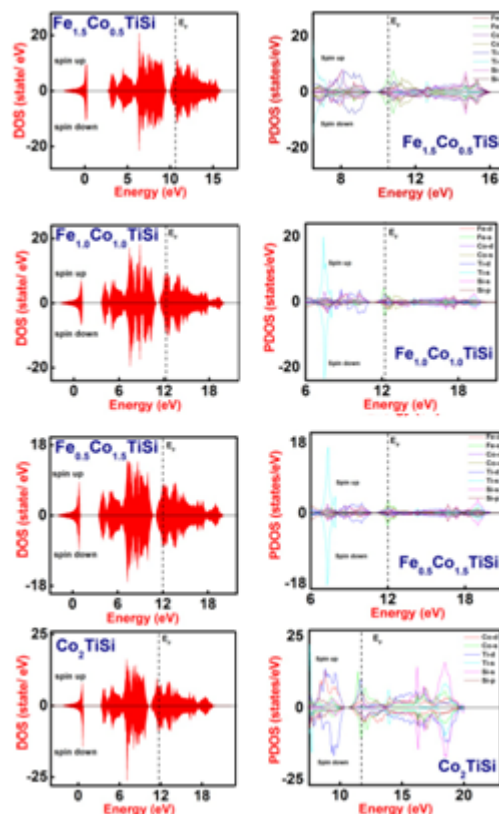
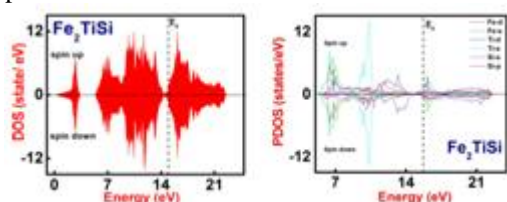
Hence, the total density of states (DOS) of Fe_{2-x}Co_xTiSi (x = 0.0, 0.5, 1.0, 1.5, 2.0) Heusler compounds computed with GGA- PBE+U scheme at normal pressure is presented in Fig. 3.2.1 (a) to (e). It is observed that Fe₂TiSi is a semiconductor material which is consistent with the results of Bhat et al. and Jong et al. [5-7]. The Co- substituted full Heusler compounds Fe₂TiSi exhibits an energy gap at the Fermi level E_F in the spin down states. The majority and

minority states are slightly shifted to a lower energy range with respect to the Fermi level. However, the change in minority states is so obvious. It is seen that energy range ~ 5 eV to ~ 7.5 eV (around the Fermi level) has a great impact on s and p state electrons of main group element. Mainly, it should be noted that peak around the Fermi level is due to the hybridization of d- state electrons. The spin flip gap (E_g) observed in $Fe_{1.5}Co_{0.5}TiSi$, $Fe_{1.0}Co_{1.0}TiSi$, $Fe_{0.5}Co_{1.5}TiSi$ and Co_2TiSi are 0.397 eV, 0.629 eV, 0.646 eV and 0.783 eV respectively.



3.2.1 Density of State and Partial Density of State at Low pressure (a) Fe_2TiSi (b) $Fe_{1.5}Co_{0.5}TiSi$ (c) $Fe_{1.0}Co_{1.0}TiSi$ (d) $Fe_{0.5}Co_{1.5}TiSi$ (e) Co_2TiSi

In order to understand the half metallicity and energy hybridization in detail, the partial density of states (PDOS) near the Fermi level of $Fe_{2-x}Co_xTiSi$ ($x=0.0, 0.5, 1.0, 1.5, 2.0$) at normal pressure is shown in Figure 3.2.2 (a) to (e). In $Fe_{2-x}Co_xTiSi$ ($x = 0.0, 0.5, 1.0, 1.5, 2.0$) compounds, Fe and Co atoms present a strong spin-splitting with antibonding states centered about ~5 eV to ~7.5 eV, in the spin states leads to the formation of spin flip gap. The conduction state in d^6 and d^7 states of Fe and Co atoms are not fully occupied in the spin down state.



3.2.2 Density of State and Partial Density of State at High pressure (a) $Fe_{1.5}Co_{0.5}TiSi$ (b) $Fe_{1.0}Co_{1.0}TiSi$ (c) $Fe_{0.5}Co_{1.5}TiSi$ (e) Co_2TiSi

As a result, an occupied 3d state in a spin down channel is mixed with sp state of main group element Ge and shows the spin flip gap. On the other side, majority spin channel shows the metallic nature. So, these d-states hybridization recognized the half metallic gap in the spin down state. Finally, the effect of substitution of Co atom in Fe site originates the appreciable changes in the electronic structure of Fe_2TiSi . This change is due to the vicinity of d- state electrons of Co-atom hybridized with Fe-atoms.

3.3 Magnetic Properties

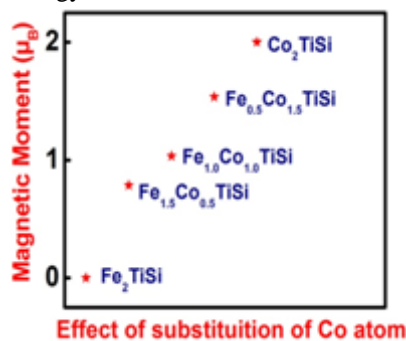
To inspect the magnetic properties of $Fe_{2-x}Co_xTiSi$ ($x = 0.0, 0.5, 1.0, 1.5, 2.0$) full Heusler alloys for their potential applications in spintronics and quantum computing, the spin polarized calculations are carried out. The ability of a spin polarization at Fermi energy (E_F) of a full Heusler alloy is calculated by the formula [9]:

$$P(\%) = \frac{\rho \uparrow(E_F) - \rho \downarrow(E_F)}{\rho \uparrow(E_F) + \rho \downarrow(E_F)} \times 100$$

where $\rho \uparrow(E_f)$ and $\rho \downarrow(E_f)$ are spin electron density of states of majority and minority states near the Fermi energy level. For the complete spin polarization, any one of the electron densities, either spin up $\rho \uparrow(E_f)$ or spin down $\rho \downarrow(E_f)$ equals zero, and it is called true half metallic behaviour. The studied full Heusler alloys $Fe_{1.5}Co_{0.5}TiSi, Fe_{1.0}Co_{1.0}TiSi, Fe_{0.5}Co_{1.5}TiSi$ and Co_2TiSi are half metals at normal pressure. In these full Heusler alloys, the electron density near the Fermi level in the minority spin channel ($\rho \downarrow(E_f)$) of all the compounds (except Fe_2TiSi) are

zero at normal pressure. Hence, it is worthwhile to note that the spin polarization of the full Heusler alloys $Fe_{1.5}Co_{0.5}TiSi$, $Fe_{1.0}Co_{1.0}TiSi$, $Fe_{0.5}Co_{1.5}TiSi$ and Co_2TiSi is 100% at the normal pressure.

For practical purposes, the ferromagnetic order of Heusler compounds must be maintained beyond ambient condition. In this regard, the total energy is calculated for non-magnetic and ferromagnetic states of $Fe_{2-x}Co_xTiSi$ ($x = 0.0, 0.5, 1.0, 1.5, 2.0$) full Heusler alloys to predict the magnetic ground state and it is observed that ferromagnetic state is more stable for these alloys except Fe_2TiSi which are accredited to their lowest energy.



Effect of substitution of Co atom

Figure 3.3.1: Magnetic moment (μ_B) versus effect of substitution of Co atom curve of $Fe_{2-x}Co_xTiSi$ ($x = 0, 0.5, 1, 1.5, 2$) full Heusler alloys

For practical purposes, the ferromagnetic order of Heusler compounds must be maintained beyond ambient condition. In this regard, the total energy is calculated for non-magnetic and ferromagnetic states of $Fe_{2-x}Co_xTiSi$ ($x = 0.0, 0.5, 1.0, 1.5, 2.0$) full Heusler alloys to predict the magnetic ground state and it is observed that ferromagnetic state is more

stable for these alloys except Fe_2TiSi which are accredited to their lowest energy. In Table 3.3.2 and 3.3.3, the total and the interstitial spin magnetic moments in the unit cell of $Fe_{2-x}Co_xTiSi$ ($x = 0.0, 0.5, 1.0, 1.5, 2.0$) full Heusler compounds using GGA- PBE and GGA- PBE+U approach are given. The implementation of Hubbard parameter (GGA PBE+U) to the host material has little impact on the magnetic moment. Interestingly, the total magnetic moment of the Fe_2TiSi alloy is zero. But when Co atom is substituted, $Fe_{1.5}Co_{0.5}TiSi$, $Fe_{1.0}Co_{1.0}TiSi$, $Fe_{0.5}Co_{1.5}TiSi$ and Co_2TiSi have the magnetic moment. Hence, the effect of doping induces the magnetism. The strong magnetism of $Fe_{2-x}Co_xTiSi$ ($x = 0.0, 0.5, 1.0, 1.5, 2.0$) in the ferromagnetic state is due to the unfilled 3d sub-shell, since the magnetic effects of electrons in the incomplete 3d orbit do not cancel each other as they are present in a complete sub-shell.

Table 3.3.2 Calculated total magnetic moment (μ_B) for $Fe_{2-x}Co_xTiSi$ ($X = 0, 0.5, 1, 1.5, 2$) in $L2_1$ structure

Compound	Method	Total Magnetic Moment (μ_B)
Fe_2TiSi	GGA- PBE	0
	GGA- PBE+U	0
$Fe_{1.5}Co_{0.5}TiSi$	GGA- PBE	0.781
	GGA- PBE+U	0.786
$Fe_{1.0}Co_{1.0}TiSi$	GGA- PBE	1.027
	GGA- PBE+U	1.034
$Fe_{0.5}Co_{1.5}TiSi$	GGA- PBE	1.507
	GGA- PBE+U	1.536
Co_2TiSi	GGA- PBE	1.987
	GGA- PBE+U	2.001 1.65 ^a , 2.00 ^b , 1.999 ^c , 1.9992 ^d

Table 3.3.3. Calculated total magnetic moment (μ_B) of individual atoms in for $Fe_{2-x}Co_xTiSi$ ($X = 0, 0.5, 1, 1.5, 2$) full Heusler alloys

Compound	Method	μ_{Fe}	μ_{Co}	μ_{Ti}	μ_{Si}	Total Magnetic Moment (μ_B)
Fe_2TiSi	GGA- PBE	0	0	0	0	0
	GGA- PBE+U	0	0	0	0	0
$Fe_{1.5}Co_{0.5}TiSi$	GGA- PBE	0.196	0.658	-0.073	0	0.781
	GGA- PBE+U	0.189	0.669	-0.072	0	0.786
$Fe_{1.0}Co_{1.0}TiSi$	GGA- PBE	0.634	0.570	-0.178	0.001	1.027
	GGA- PBE+U	0.644	0.578	-0.188	0	1.034
$Fe_{0.5}Co_{1.5}TiSi$	GGA- PBE	0.807	0.837	-0.154	0.017	1.507
	GGA- PBE+U	0.827	0.848	-0.155	0.016	1.536
Co_2TiSi	GGA- PBE	0	1.996	-0.040	0.031	1.987
	GGA- PBE+U	0	2.004 1.03 ^a , 0.988 ^b , 1.180 ^c	-0.032 -0.02 ^a , 0.032 ^b , -0.1723 ^c	0.029 0.007 ^b , 0.0004 ^c	2.00 ^a , 1.999 ^b , 1.9992 ^c

3.4 Mechanical Properties

The elastic constants and elastic moduli are fundamental materials parameters providing detailed information on the mechanical properties of materials. The knowledge of these data may be used to predict mechanical behavior in many different situations. The parameters σ_{mn} and ϵ_{pr} are symmetric and have only 6 independent elements, hence the number of 81 elastic constant is reduced to 21

by symmetry arguments. The elastic energy density U , which is defined as the total energy per volume, is obtained from the stress tensor (force per unit area) by integration of Hooke's law

$$U = \frac{E}{V} = \frac{1}{2} C_{mnp} \epsilon_{mn} \epsilon_{pr}$$

The strain tensor has been considered as a tensor of order two of the form

$$\varepsilon = \begin{pmatrix} 1 + e_{xx} & \frac{1}{2} e_{xy} & \frac{1}{2} e_{xz} \\ \frac{1}{2} e_{yx} & 1 + e_{yy} & \frac{1}{2} e_{yz} \\ \frac{1}{2} e_{zx} & \frac{1}{2} e_{zy} & 1 + e_{zz} \end{pmatrix}$$

In the convenient matrix-vector notation, the 6 independent elements of stress and strain are represented as vectors (denoted here as ε_i and ε_j with i, j running from 1 ... 6 according to the sequence xx, yy, zz, yz, xz, xy) and the fourth order tensor C_{mnpq} can be rewritten as a 6x6 matrix c_{ij} , then

$$U = \frac{E}{V} = \frac{1}{2} C_{ij} \varepsilon_i \varepsilon_j$$

Taking into account additional symmetry arguments imposed by the crystal lattice, the number of elastic constants further decreases. In particular, for a cubic lattice only three independent elastic constants, c_{11}, c_{12}, c_{44} are sufficient. In order to calculate the elastic constants of a structure, a small strain is applied on to the structure and its stress is determined. The energy of a strained system [1, 2] can be expressed in terms of the elastic constants C_{ij} as:

$$E(V, \varepsilon_i) = E(V_0, 0) + V_0 \sum_{i=1}^6 \sigma_i \varepsilon_i + \frac{V_0}{2} \left(\sum_{i,j=1}^6 C_{ij} \varepsilon_i \varepsilon_j \right) + O(\{\varepsilon_i^3\}) \dots$$

The elasticity tensor has three independent components (C_{11}, C_{12}, C_{44}) for cubic crystals. A proper choice of the set of strains $\{\varepsilon_i, i=1,2,\dots,6\}$, in Eq.(5.6) leads to a parabolic relationship between $\Delta E/V_0$ ($\Delta E \equiv E-E_0$) and the chosen strain. Such choices for the set $\{\varepsilon_i\}$ and the corresponding form for ΔE are shown in Table 5.1 for cubic lattices [3]. For each lattice structure, the lattice was strained by 0%, $\pm 1\%$, and $\pm 2\%$ to obtain their total minimum energies $E(V)$. These energies and strains were fitted with the corresponding parabolic equations of $\Delta E/V_0$ as given in Table 3.4.1 to yield the required second-order elastic constants. While computing these energies all atoms are allowed to relax with the cell shape and volume fixed by the choice of strains $\{\varepsilon_i\}$.

The independent elastic constants should satisfy the Born-Huang elastic stability criteria [4] given by: $C_{44} > 0, C_{11} > |C_{12}|, C_{11} + 2C_{12} > 0$ for the stable cubic structure. The strain energy $1/2 C_{ij} \varepsilon_i \varepsilon_j$ of a given crystal in equation (5.8) must always be positive for all possible values of the set $\{\varepsilon_i\}$; for the crystal to be mechanically stable. As per this work the calculated elastic constants are positive for all the phases and obey the necessary mechanical stability conditions. The bulk modulus (B) and shear modulus (G) for the cubic crystals are determined using Voigt – Reuss – Hill (VRH) averaging scheme [5-7].

Table 3.4.1: Strain combinations in the strain tensor for calculating the elastic constants of cubic structures

Cubic crystals		
Strain	Parameters (unlisted $\varepsilon_i=0$)	$\Delta E/V_0$
1	$\varepsilon_1=\varepsilon_2=\delta, \varepsilon_3=(1+\delta)^2-1$	$3(C_{11}-C_{12})\delta^2$
2	$\varepsilon_1=\varepsilon_2=\varepsilon_3=\delta$	$(3/2)(C_{11}+2C_{12})\delta^2$
3	$\varepsilon_6=\delta, \varepsilon_3=\delta^2(4\delta^2)^{-1}$	$(1/2)C_{44}\delta^2$

Young modulus refers to longitudinal stress and strain. The shear (or rigidity) modulus is the tangential force per unit area divided by the angular deformation. The ratio of the lateral strain to the longitudinal strain is known as Poisson’s ratio. It was first introduced by Simeon-Denis Poisson (1781-1840). Anisotropic denotes a medium in which certain physical properties are different in different directions.

The mechanical properties such as Young’s modulus (E), shear modulus (G) and Poisson’s ratio (ν) are important physical quantities, especially for engineering and technological applications. The hardness of the polycrystalline material can be investigated by computing the Kleinman parameter. These parameters are calculated using the following relations [8]:

$$E = \frac{9BG}{3B + G}$$

$$\nu = \frac{C_{12}}{C_{11} + C_{12}}$$

$$\zeta = \frac{C_{11} + 8C_{12}}{7C_{11} + 2C_{12}}$$

$$A = \frac{2C_{44}}{C_{11} - C_{12}}$$

The calculated mechanical parameters for $Fe_{2-x}Co_xTiSi$ ($X=0, 0.5, 1, 1.5, 2$) with considered phases of

$L2_1$ structure using GGA-PBE and GGA-PBE+U is presented in Tables 3.4.2. Young’s modulus is often used to provide a measure of stiffness of a solid, i.e., larger the value of Young’s modulus, stiffer is the material. The computed Young’s modulus values indicate that Fe_2TiSi is the stiffest material. The Poisson’s ratio is associated with the volume change during uniaxial deformation, and it reflects the stability of the crystal against shear. The $\nu=0.25$ and 0.5 are the lower and upper limits, respectively, for central force in solids [7]. It is observed that Poisson’s ratio for $Fe_{2-x}Co_xTiSi$ ($x=0, 0.5, 1, 1.5, 2$) full Heusler alloys is in the range of $0.3-0.4$, which indicates that the bonding is more ionic in nature.

The ratio of bulk modulus to shear modulus (B/G) is used to estimate the brittle or ductile nature of materials. A high B/G value is associated with ductility, while a low B/G value corresponds to the brittle nature. The critical value which separates ductile and brittle materials is about 1.75. The ratios of B/G values of these full Heusler compounds is greater than the critical value 1.75 indicating that they are ductile materials in their stable $L2_1$ phase. The Zener anisotropy factor (A) measures the degree of anisotropy in the solid structure. The value of $A=1$, represents completely elastic isotropy, while values smaller or larger than 1 measure the degree of elastic anisotropy. The calculated

values of A predict that all the alloys are not close to the value of 1, which indicates that these full Heusler alloys has complete elastic anisotropy.

The Debye temperature (θ_D) is an important parameter closely related to many physical properties of materials, such as specific heat, elastic constants and melting temperature. The Debye temperature is calculated from the elastic constants data using average sound velocity v_m by the following common equation [8]:

$$\theta_D = \frac{\hbar}{k_B} \left[6\pi^2 n \frac{N_{AP}}{M} \right]^{1/3} v_m$$

$$v_m = \left[\frac{1}{3} \left(\frac{2}{v_t^3} + \frac{1}{v_l^3} \right) \right]^{-1/3}$$

where

Table 3.4.2 Calculated elastic constants C_{11} , C_{12} , C_{44} (GPa) for $Fe_{2-x}Co_xTiSi$ ($x=0, 0.5, 1, 1.5, 2$) in $L2_1$ structure. Total energy E (eV), formation enthalpy ΔH (KJ/mol), bulk modulus B_0 (GPa) and its derivative B_0' for $Fe_{2-x}Co_xTiSi$ ($x=0, 0.5, 1, 1.5, 2$) in $L2_1$ structure

	Method	C_{11}	C_{12}	C_{44}	B	G	B/G	E	ν	A	θ_D (K)
Fe_2TiSi	GGA- PBE	436.73	128.89	87.84	231.50	114.27	2.0259	294.39	0.3099	0.5707	748.69
	GGA- PBE+U	428.59	124.83	82.47	226.08	110.23	2.0509	284.47	0.3121	0.5429	727.91
		442.92 ^a , 457 ^b , 462.4 ^c	130.80 ^a , 119 ^b , 124.5 ^c	161.16 ^a , 152 ^{b,c}	232.1 ^b , 237.1 ^c	158.7 ^b , 158.6 ^c	1.463 ^b , 1.496 ^c	387.7 ^b , 389 ^c	0.221 ^b		
$Fe_{1.5}Co_{0.5}TiSi$	GGA- PBE	335.05	156.12	105.23	215.76	98.92	2.1811	257.43	0.3225	1.1761	703.78
	GGA- PBE+U	342.99	144.61	110.37	210.74	105.89	1.9901	272.11	0.3068	1.1127	729.72
$Fe_{1.0}Co_{1.0}TiSi$	GGA- PBE	369.76	153.56	78.65	225.63	90.43	2.4950	239.32	0.3434	0.7275	672.10
	GGA- PBE+U	313.86	158.35	99.91	210.19	91.05	2.3085	238.68	0.3316	1.2849	677.96
$Fe_{0.5}Co_{1.5}TiSi$	GGA- PBE	338.28	160.94	96.04	220.05	93.09	2.3638	244.76	0.3353	1.0831	685.73
	GGA- PBE+U	310.89	159.36	98.89	209.87	89.64	2.3412	235.40	0.3338	1.3052	661.45
Co_2TiSi	GGA- PBE	372.87	143.82	87.78	220.17	98.47	2.2359	257.10	0.3265	0.7664	696.80
	GGA- PBE+U	344.77	128.75	75.37	200.75	88.43	2.2701	231.32	0.3290	0.6978	650.05

4. Conclusion

The electronic structure and magnetic properties have been calculated using the first principles augmented plane waves (FP-APW) method for the $Fe_{2-x}Co_xTiSi$ ($x=0.0, 0.5, 1.0, 1.5, 2.0$). The spin polarized calculations showed that the Co_2TiSi Heusler compound is half-metallic with a magnetic moment of 2 μ_B . $Fe_{2-x}Co_xTiSi$ ($x=0.0, 0.5, 1.0, 1.5, 2.0$) revealed that the Full Heusler alloys have a perfect half-metallic character and 100% polarization which making them as good candidate in spintronics applications. The values of B/G indicates that all the $Fe_{2-x}Co_xTiSi$ ($x=0, 0.5, 1, 1.5, 2$) full Heusler alloys are ductile in nature and also the Poisson's ratio for full Heusler alloys is in the range of 0.3–0.4, which indicates that the bonding is more ionic in nature. The computed Young's modulus values indicate that stiffest material. The value of anisotropy factor indicates that this full Heusler alloy has complete elastic anisotropy. The high value of the Debye temperature for Fe_2TiSi indicates its thermal conductivity.

5. Acknowledgment

This work is entirely supported by Vienna ab initio simulation package under the guidance of Dr.R.Rajeswarapalanichamy, Associate professor/Physics

$$v_l = \left(\frac{B + 0.75G}{\rho} \right)^{1/2} \text{ and } v_t = \left(\frac{G}{\rho} \right)^{1/2}$$

are the velocities of longitudinal and transverse sound waves respectively. The calculated Debye temperature values for $Fe_{2-x}Co_xTiSi$ ($X=0, 0.5, 1, 1.5, 2$) using GGA PBE are listed in Tables 3.4.2 respectively.

For materials, usually, the higher Debye temperature indicates the larger thermal conductivity and microhardness. From Table 3.4.2, it is seen that Fe_2TiSi has the highest Debye temperature (748.69 K using GGA- PBE and 727.91 K using GGA- PBE+U) which exhibits the strong covalent bond and high thermal conductivity among the studied $Fe_{2-x}Co_xTiSi$ ($x=0, 0.5, 1, 1.5, 2$) full Heusler alloys.

department at Nadar Mahajana Sankam S.Vellasamy Nadar College (An Autonomous Institution), Madurai.

References

- [1] M. Meinert, M. P. Geisler, J. Schmalhorst, U. Heinzmann, E. Arenholz, Walid Hetaba, M. S. Pollach, A. Hutten, and G. Reiss, Phys. Rev. B **90** (2014) 085127.
- [2] A. I. Voronin, V. Yu. Zueva, D. Yu. Karpenkov, D. O. Moskovskikh, A. P. Novitskii, H. Miki, and V. V. Khovaylo, Semiconductors, **51** (2017) 891.
- [3] K.H.J. Buschow, P.G. van Engen and R. Jongebreur, J. Magn. Mater. **38** (1983) 1.
- [4] S. Chaudhuri, P. A. Bhohe and A. K. Nigam, AIP Conference Proceedings **1832** (2017) 110027 [5] I. H. Bhat, T. M. Bhat and Dinesh C. Gupta, J. Phys. Chem. Solids **119** (2018) 251.
- [5] J.Y. Jong, J. Zhu, S. I. Pak, and G. H. Sim, J. Electron. Mater. **45** (2016) 5104.
- [6] J.Y. Jong, J.Yan, J.C. Zhu, and C. J. Kim, J. Electron. Mater. DOI: 10.1007/s11664-017-5564-z.
- [7] S.Yabuuchi, M. Okamoto, A. Nishide, Y. Kurosaki, and J. Hayakawa, Applied Physics Express **6** (2013) 025504.

- [8] H. C Kandpal, G. H Fecher and C. Felser, J. Phys. D: Appl. Phys. **40** (2007) 1507.
- [9] V. Sharma, A.K.Solanki, A.Kashyap, J. Magn. Magn. Mater. **322** (2010) 2922.
- [10] M. K. Zayed, A.A. Elabbar and O.A. Yassin, J. Alloys Compd. **737** (2018) 790.
- [11] J. P. Perdew, S. Burke, Phys. Rev. B **54** (2004) 16533.
- [12] P. E. Blochl, Phys. Rev. B **50** (1994) 17953.
- [13] G. Kresse, J. Joubert, Phys. Rev. B **59** (1999) 1758.
- [14] G. Kresse, J. Hafner, Phys. Rev. B **47** (1993) 558.
- [15] G. Kresse, J. Furthmuller, Comput. Mater. Sci. **6** (1996) 15.
- [16] J. P. Perdew, S. Burke, Phys. Rev. Lett. **78** (1997) 1396.
- [17] H. J. Monkhorst, J. D. Pack, Phys. Rev. B **13** (1976) 5188.